PHYSICAL REVIEW B VOLUME 24, NUMBER 9 1 NOVEMBER 1981

Electron-spin-resonance studies of a family of organic conductors

H. J. Pedersen* and J. C. Scott†
Laboratory of Atomic and Solid State Physics and Material Science Center, Cornell University, Ithaca, New York 14853

K. Bechgaard
Department of General and Organic Chemistry, H. C. Orsted Institute, University of Copenhagen, Universitetsparken 5, DK-2100 Copenhagen, Denmark
(Received 24 February 1981)

The family of organic conductors $(TMTSF)_2X$, where TMTSF is tetramethyltetraselenafulvalene and $X = PF_6^-$, AsF_6^-, SbF_6^-, NO_3^-, or BF_4^-, has been studied using electron-spin-resonance techniques. Linewidth, g-tensor, and susceptibility data, as functions of temperature and orientation, are reported. The results imply an overall similarity among the members of the family, but some striking differences in detail are observed. We introduce a phenomenological model which explains some of the features of the linewidth anisotropy and temperature dependence. The paper includes a discussion of the metal-insulator transitions in terms of a spin-density-wave description.

I. INTRODUCTION

The family of materials $(TMTSF)_2X$, where TMTSF is the organic donor tetramethyltetraselenafulvalene and X is an inorganic anion such as PF_6^-, AsF_6^-, SbF_6^-, NO_3^-, or BF_4^-, is proving to be a remarkable series of organic conductors. Room-temperature conductivities[1] are of the order $10^3\ \Omega^{-1}cm^{-1}$, with a two-orders-of-magnitude increase on cooling. The metal-insulator transition temperatures[1] are relatively low, lying in the range 10–20 K (except the BF_4^- compound which changes phase at 38 K). Superconductivity has been observed[2–5] at 1 K under pressure of order 10 kbar. There is a growing body of evidence[6–10] that the nature of the metal-insulator transition, at least in the hexafluorophosphate, may not be, as initially assumed, a Peierls instability, but rather has some magnetic origin such as a spin-density wave.

A comprehensive study of this series of compounds is particularly appealing because of the number of members, differing only in the anion. Although a complete set of crystal structures is not yet available, the similarity of external morphology, of electrical conductivity, of thermopower and of the ESR spectra reported here strongly suggest that the materials are more or less isostructural. In the PF_6^- complex there is known[1,11] to be only one chain of organic TMTSF molecules within the unit cell. This structural feature persists in the other cases,[12] and the analysis of data should be much simpler than for the two-chain organic conductors.[13] The different inorganic counterions can be expected to lead to relatively subtle changes in intrachain spacing (i.e., bandwidth), interchain spacing and setting angle (i.e., transverse hopping integral and Coulomb interaction), polarizability (i.e., screening), and molecular symmetry (i.e., lattice dynamics). Thus, while we do not wish to imply that organic metals are in any way "simple," it might be possible perhaps for the first time, to explore in a systematic way, the effects of various kinds of interaction (intrachain and interchain Coulomb, electron-phonon, transverse hopping) on the one-dimensional electron gas.

In this paper we report the ESR spectroscopy of the family of materials $(TMTSF)_2X$ where $X = PF_6^-$, AsF_6^-, SbF_6^-, NO_3^-, and BF_4^-. The temperature dependence and anisotropy of the ESR linewidth, g factor, and susceptibility have been obtained. The gross spectral features of all the materials are similar, but, as expected on the basis of the discussion in the preceding paragraph, there are many differences in detail. While there are still insufficient other data available to permit a systematic analysis, our results indicate that it will fruitful to study the series of materials as a whole and not to concentrate on individual members of it.

The paper is arranged as follows: in Sec. II we outline the experimental method and the data analysis, including a discussion of Dysonian line shapes in quasi-one-dimensional conductors; the results of the experiment are given in Sec. III, beginning with a description of the generalities then passing to the features which seem peculiar to a given material or subset of materials; Sec. IV is a discussion and includes an analysis of the linewidth, its temperature dependence and anisotropy on the basis of a new phenomenological approach; there is also a comparison of the behavior near the respective metal-insulator transitions; finally, in Sec. V, we give a summary, our conclusions and some conjectures.

II. EXPERIMENTAL

A. Sample preparation

Single crystals of the $(TMTSF)_2X$ compounds were obtained by the following procedure: A $10^{-3}M$ solution of gradient-sublimed TMTSF (Ref. 14) in dry deoxgenated spectrograde CH_2Cl_2 containing the appropriate supporting electrolyte (R_4NX) in $0.1-0.5M$ concentration was oxidized at a platinum anode at constant current (5 μA, 0.25 cm^2 Pt) in a sealed cell to approximately 70% conversion. The resulting black crystals were harvested, washed twice with cold CH_2Cl_2 and vacuum dried. No special precautions were taken to protect the crystals except to store them in sealed containers. Microanalysis (C,H,N) in all cases indicated perfect 2:1 stoichiometry.

B. ESR spectroscopy

Spectra were obtained by using a home-built X-band homodyne spectrometer of standard design. The klystron frequency ($\sim$9.4 GHz) was stabilized using an independent high-Q cavity in the wavemeter mode, and was measured with a Hewlett-Packard model 5245L frequency counter. Stability and precision were on the order of 10 kHz. The double-arm spectrometer was tuned for absorption, a condition which simultaneously minimizes klystron amplitude noise. The maximum power which could be delivered to the sample cavity was on the order of 200 mW. The sample cavity was a Brucker B-ER400XUR Universal Resonator, in its TE_{102} mode with a Q of order 7000. Hence, the maximum radio frequency field at the sample was $H_1^{\max} \sim 0.4$ G. Normal operating levels were -30 to -10 dB from the maximum, which has only used to make saturation studies.

Samples were mounted on a nylon holder inside a standard 4-mm spectrosil quartz ESR tube and surrounded by 1-atm He exchange gas. Cooling and temperature control were achieved using an Oxford Instruments ESR9 continuous-flow helium system. This apparatus uses an iron: gold-Chromel thermocouple which was checked using a Curie-like dilute spin system and found to be accurate to within 1 K at 20 K provided that a sufficient helium-flow rate was maintained. The sample was located at the central antinode of the H_1 field in the cavity. H_1 was vertical and the static field H_0 horizontal. The sample could be rotated round a vertical axis using a homemade goniometer.

The static field was obtained with a Varian 6-in. magnet and V2200A power supply, and controlled with a Varian Fieldial Mark I (Hall effect) regulator. The absolute magnitude of the magnetic field at the sample position was obtained by observing the resonance of a diphenylpicrylhydrazyl (DPPH) sample, and using the frequency counter. For the most accurate g-value determination the sample and a DPPH marker were put simultaneously into the cavity.

The magnetic field was modulated at 1400 Hz using the coils attached to the Bruker cavity. Standard lock-in detection methods were employed and the first derivative signal, $S(H)$ was recorded and digitized (1024 points) with a Nicolet model 1170 signal averager. The digital data were subsequently transmitted to a Prime 400 computer for analysis.

The data were fit in general to the expression for the derivative of a Lorentzian absorption line

$$S = \frac{-2A(H-H_c)\Gamma^2}{[(H-H_c)^2+\Gamma^2]^2} , \tag{1}$$

where A is the amplitude, Γ is the width, and H_c is the center field. At high temperatures, where all lines were broad ($\gtrsim$100 G) it was necessary to include a sloping baseline in the fit. Such a fit was found to lie within the noise to fields $(H-H_c)$ up to 10 (at 300 K) or 20 (near 20 K) times the linewidth.

The susceptibility results given below were obtained as the product $A\Gamma$. The absolute magnitude of each room-temperature susceptibility was measured by direct comparison with tetrathiofulvalene-tetracyanoquinodimethane (TTF-TCNQ) (Refs. 15 and 16) which also has a Lorentzian line.[16,17]

C. Asymmetric line shapes

In all measurements with the static field, H_0, parallel to the highly conducting axis, and in some samples with a transverse field at low temperature an asymmetric, i.e., Dysonian,[18] line was observed. Such behavior is easily understood in terms of the eddy currents which circulate in the plane perpendicular to the radio frequency field, H_1, and hence sample two components of the conductivity tensor. If the conductivity is sufficiently high the currents will shield the rf radiation and a skin-depth picture must be used. In this section we shall show that the conductivity tensors of the $(TMTSF)_2X$ family are such that the spin motion may be neglected (i.e., the time for an electron to diffuse through the skin depth, T_D is very long compared to the relaxation time, T_2) and that the signal is therefore proportional to a linear combination of the real and imaginary susceptibilities.[19]

Consider the electromagnetic radiation incident on the sample shown in Fig. 1. H_0 is along the z axis, H_1 along x and we consider separately the radiation fields having electric vectors polarized along the y and z axes. The penetration of the wave with z polarization is determined by the conductivity σ_z. (We assume for simplicity that the conductivity tensor is aligned with the system of axes chosen.) Hence the

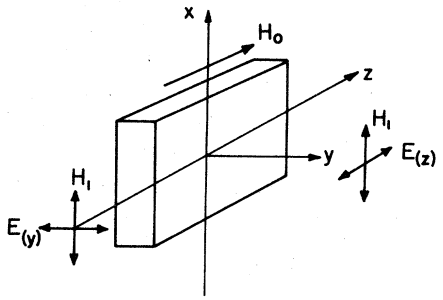

FIG. 1. Sample and field geometry used in the discussion of Dysonian line shapes.

skin depth for propagation in the $\pm y$ direction, (cgs)

$$\lambda_y = c/(2\pi\sigma_z\omega)^{1/2} \ . \tag{2}$$

On the other hand, the time for an electron to diffuse through this skin depth is determined by the conductivity σ_y. For a "worst case" analysis, the diffusion is via band motion with scattering and therefore the shortest diffusion time

$$T_{D_y} = \lambda_y^2/D_y = ne^2c^2/2\pi\sigma_y\sigma_z\omega W_y \ , \tag{3a}$$

where D_y is the diffusion constant and W_y is the bandwidth for propagation in the $\pm y$ directions. (Use of the Einstein relation gives a longer diffusion time.) Similarly for the wave polarized along y

$$T_{D_z} = ne^2c^2/2\pi\sigma_y\sigma_z\omega W_z \ . \tag{3b}$$

To estimate this time when the z axis is that of highest conductivity and y is next highest, take $\sigma_z = 10^5\ \Omega^{-1}\text{cm}^{-1}$, $\sigma_y = 10^2\ \Omega^{-1}\text{cm}^{-1}$ (their highest values,[1,20] attained at 20 K in $TMTSF_2PF_6$) and $W_z = 1$ eV. Then $T_{D_z} \gtrsim 10^{-3}$ sec. The minimum linewidth is of order 5 G, hence $T_2 \lesssim 10^{-7}$ sec. Therefore, we conclude that the condition $T_D >> T_2$ is very well satisfied over the entire temperature range of measurement.

The static spin (or Bloembergen[21]) limit of Dyson's skin-depth theory[18] therefore applies. In this situation each electron sees an H_1 with a phase which is constant in time but spatially varying through the sample. The effect on the spectrometer signal is to mix the real and imaginary parts of the susceptibility. Since the rf field is also attenuated within the sample the magnitude of the signal is lowered by an amount which depends on the geometry of the sample and its depolarization factors. Since it is impossible to solve in full the boundary-value problem for an arbitrarily shaped crystal[19] (most samples were needles of irregular cross section) we have chosen to treat the signal amplitude as an additional fitting parameter, i.e., to fit the signal to the form

$$S = \frac{\partial}{\partial H}(a\chi' + b\chi'') \ , \tag{4}$$

where χ' and χ'' are the real and imaginary susceptibilities associated with a Lorentzian absorption profile.

III. RESULTS

A. Temperature dependence of the linewidth

In this subsection, as in the other parts of this section, we shall describe first the features which are common to all members of the series. Then we shall point out the details in which they differ.

The temperature dependence of the linewidth, $\Gamma(T)$, for all five compounds is shown in Figs. 2–4. The room-temperature widths are all in the range 150–300 G. Below room temperature the widths decrease, approximately linearly with temperature down to about 100 K, at which point there is a knee and below which the temperature dependence is faster,

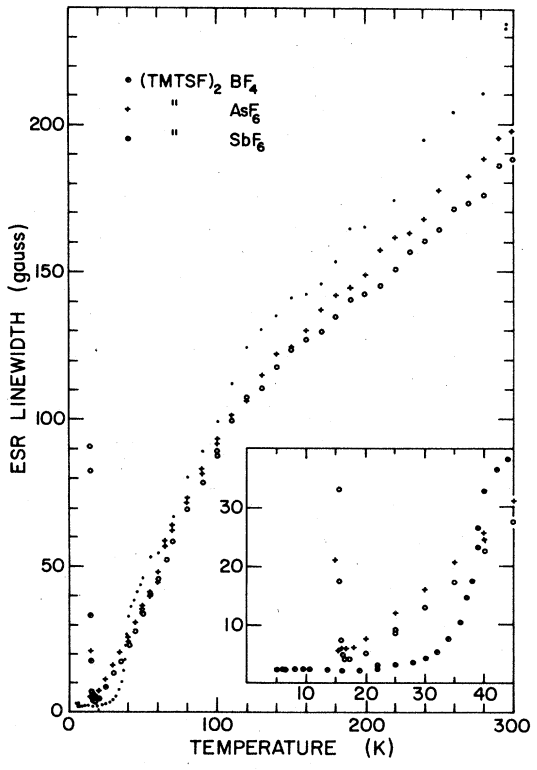

FIG. 2. Linewidth of three of the compounds studied. The field H_0 was transverse to the needle (highly conducting) axis. The inset is an expansion of the low-temperature region.

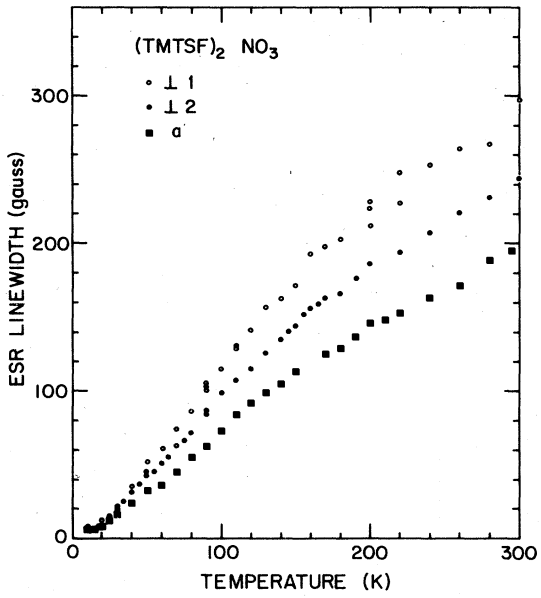

FIG. 3. Linewidth of $(TMTSF)_2NO_3$ for three field orientations. The *a* direction is the conducting axis. "⊥2" is the direction normal to the broad face of the crystal.

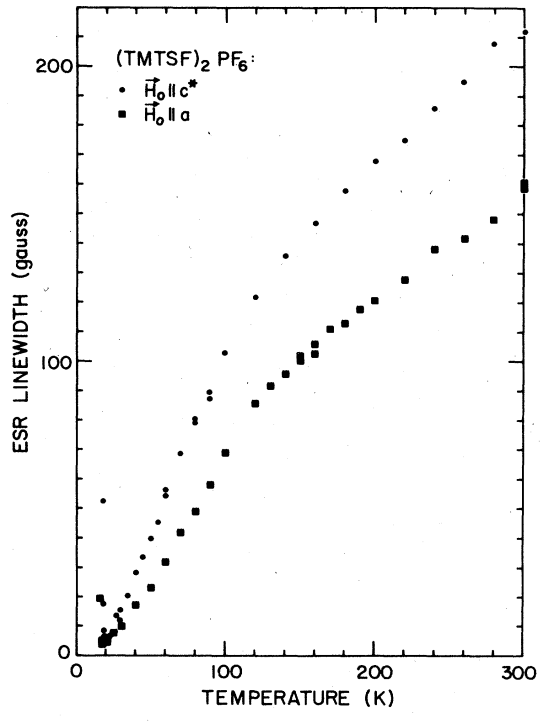

FIG. 4. Linewidth of $(TMTSF)_2PF_6$ for parallel and perpendicular field orientation. The linewidth for $\vec{H} \parallel c^*$ is roughly midway between the extrema in the perpendicular plane. (See Ref. 6.)

but still decreasing with decreasing T. The width then seems to level off in the temperature range just above the metal-insulator transitions.

The most striking difference in behavior among the various materials occurs in the region of the respective metal-insulator transitions (T_{MI}). In the case of the hexafluorides (PF_6^-, AsF_6^-, and SbF_6^- in Figs. 2 and 4) the linewidth increases abruptly, a factor of order 10, as the temperature is lowered by 1 or 2 K. The linewidth in the nitrate (Fig. 3) shows no dramatic behavior in the neighborhood of its metal-insulator transition. Finally, at the much higher transition in the perfluoroborate the linewidth falls sharply within a few kelvin below T_{MI}, to a limiting value of 2 G, i.e., $\frac{1}{20}$th of its value just above T_{MI}.

Thus, already from the linewidth we can see that, while the overall features at high temperature are quite similar, there are distinct differences among the materials, especially in the region of their transition temperatures.

B. Linewidth anisotropy

It is clear from Figs. 3 and 4 that there is considerable anisotropy in the linewidth. We decided to examine the two materials shown there (the NO_3^- and PF_6^- complexes) in more detail. The linewidth of $(TMTSF)_2NO_3$ versus the static-field direction in the plane transverse to the conducting axis is shown, for various temperatures, in Fig. 5. Our data for the hexafluorophosphate, which has similar behavior, have been published previously.[6]

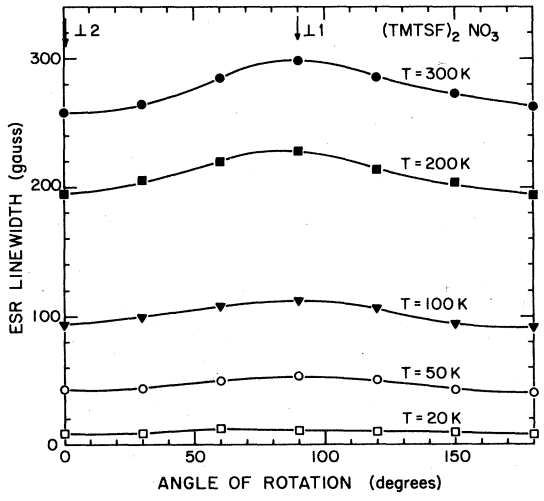

FIG. 5. Linewidth anisotropy of $(TMTSF)_2NO_3$ in the perpendicular plane.

The anisotropy may be summarized as follows: the linewidth for static field along the highly conducting axis is 30% to 50% less than that in the perpendicular plane; comparison with the g-tensor data (to be discussed below) shows that, in the transverse plane, the linewidth is largest for the same direction the g shift is largest; the temperature dependence of the relative anisotropies are rather weak, i.e., all components of linewidth have roughly the same temperature dependence, including the region of the transition.

C. Susceptibility

The absolute magnitudes of the room-temperature susceptibilities are given in Table I. These values were measured, as discussed in Sec. II B, by comparison with TTF-TCNQ. The temperature dependences of the susceptibilities, $\chi_{ESR}(T)$, of all five materials are shown in Figs. 6 and 7, the absolute magnitudes being obtained by normalization to the room-temperature value of each material. To within experimental accuracy the susceptibility is isotropic in static-field orientation. The data shown are for field directions transverse to the conducting axis.

Well above the metal-insulator transitions the general behavior is for the susceptibilities to increase rather weakly with temperature, in the manner of most of the highly conducting, nondisordered, segregated-stack organic metals which have been studied to date.[13,22–26] It is worth commenting that, in this temperature range, the static susceptibility[8] (corrected for core diamagnetism) of $(TMTSF)_2PF_6$ follows precisely $\chi_{ESR}(T)$, and, therefore, we conclude that the ESR signal corresponds to the entire conduction-electron susceptibility. The similar

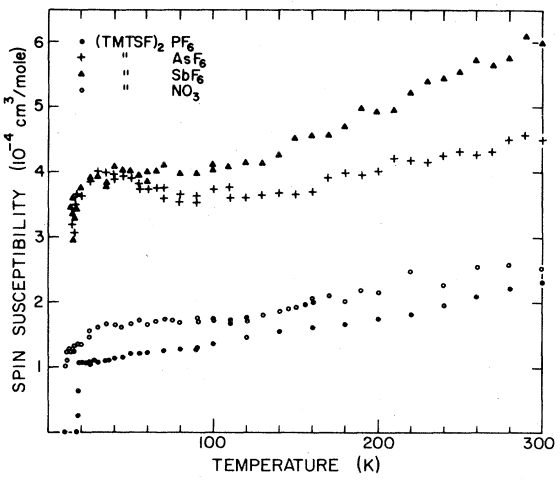

FIG. 6. ESR susceptibilities of four of the compounds.

overall behavior for the other materials strongly suggests that the same holds true for them, but this is a question which remains to be conclusively proved.

In the case of the nitrate, hexafluoroarsenate, and antimonate there is a gradual roll-off of the susceptibility between about 40 K and T_{MI}. This is the same region in which the line shape, even in the transverse plane, is becoming asymmetric in these materials. The reduction should, therefore, be attributed to skin-depth limiting of the radiation field within the sample (see Sec. II C) and not to intrinsic effects.

At the metal-insulator transitions, as obtained by independent transport measurements, the ESR intensity disappears very rapidly for all the materials. Note that this is *not* merely a consequence of reduced signal due to the increased breadth of the line; the ESR

TABLE I. Properties of the various members of the $(TMTSF)_2X$ family. T_{MI}^{ESR} is identified as the midpoint of the rapid decrease in ESR intensity. The bandwidth is calculated assuming a Pauli susceptibility. The given range reflects the temperature dependence of the susceptibility in the metallic state.

Anion	$\chi_{ESR}(300\ K)$ (10^{-4} cm^3/mole)	T_{MI}^{ESR} (K)	$\frac{\chi_{ESR}(T_{MI}^+)}{\chi_{ESR}(300)}$	Bandwidth (eV)
PF_6^-	2.3 ± 0.2	18 ± 2	0.50 ± 0.05	0.25–0.50
AsF_6^-	4.5 ± 0.4	15	0.85 ± 0.05	0.13–0.15
SbF_6^-	6.0 ± 0.5	15	0.65 ± 0.05	0.10–0.15
NO_3^-	2.5 ± 0.3	10	0.65 ± 0.05	0.23–0.35
BF_4^-	6 ± 2	40	0.60 ± 0.05	0.1–0.2

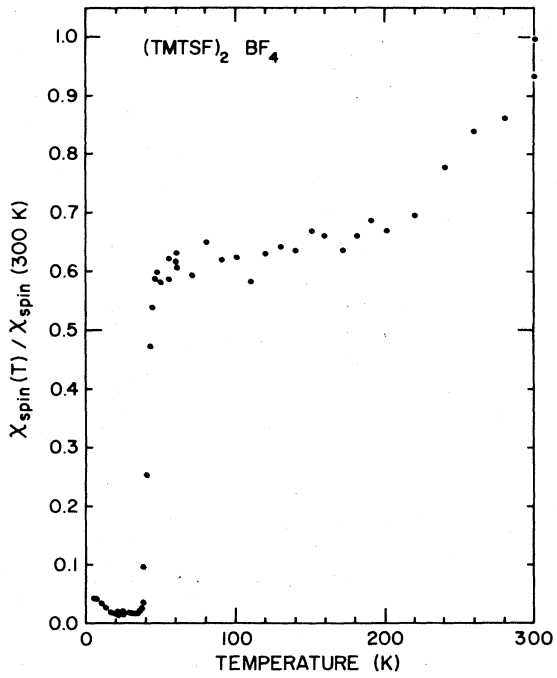

FIG. 7. ESR susceptibility (normalized to its room-temperature value) of $(TMTSF)_2BF_4$. The absolute uncertainty in χ_{ESR} is rather large for this compound. (See Table I.)

susceptibility which we discuss is the *integrated* intensity (i.e., the product $A\Gamma$). The width of the transition region, i.e., the temperature range over which χ_{ESR} drops from its relatively constant high-temperature value to zero, is of the order of 1–2 K, the same range over which the linewidth increases in the hexafluorides, and decreases in the perfluoroborate. The center of this range is used to define a T_{MI} as given in Table I.

Again, there are small differences in detail among the susceptibilities of the various materials. The ratio of the susceptibility just above the transition to that at room temperature varies from 50% for the phosphate to 85% for the arsenate. Indeed the latter material is unusual in that it has a broad minimum in its susceptibility near 100 K. Since the linewidth of the BF_4^- compound decreases below its metal-insulator transition we were able to follow it to very much lower temperature (Fig. 7). The signal never completely disappears but rather gradually evolves into a Curie tail. The perpendicular g value although showing a distinct minimum near 40 K, varies continuously and only by a few parts in 10^3 throughout the entire temperature range indicating that the paramagnetic defects reside on the TMTSF cations.

D. g tensor

The principal components of the g tensor for all materials are typical of those for the TMTSF radical cation.[27] As an example we show the data for $(TMTSF)_2NO_3$ in Fig. 8. We have shown previously,[6] for $(TMTSF)_2PF_6$ whose crystal structure is known, that the principal axes of the g tensor are aligned, to within our accuracy, with the molecular axes. The values for the hexafluorophosphate (at room temperature) and for the nitrate are summarized in Table II, and are comparable to the values obtained on other TMTSF salts by Walsh *et al.*[27] The largest g value corresponds to the long axis of the organic molecule, which is rotated 26° from the c^* axis of the PF_6^- structure.[1,11] The intermediate g value lies along the short axis of the molecule. The minimum g is perpendicular to the molecular plane and hence (nearly) along the conducting direction. In $(TMTSF)_2NO_3$ g_{max} occurs when H_0 is perpendicular to the largest flat face of the lathelike crystal. Therefore, we are led to conclude that the crystal packing of the nitrate is different from that of the phosphate, the molecular axis being parallel to a major direction of the reciprocal lattice.

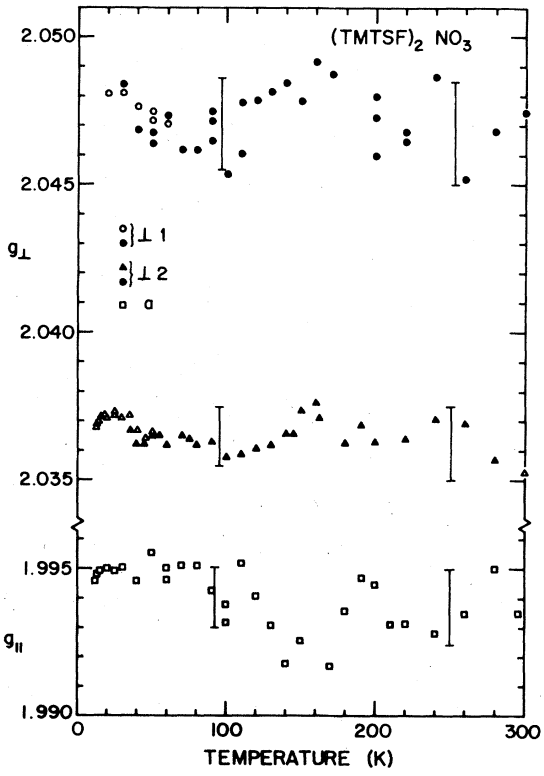

FIG. 8. Temperature dependence of the principal components of the g tensor of $(TMTSF)_2NO_3$. Solid symbols are data analyzed according to Eq. (1), open symbols Eq. (2).

TABLE II. Comparison of the principal components of the g tensors of $(TMTSF)_2NO_3$ and $(TMTSF)_2PF_6$.

	NO_3^-	PF_6^-
g_{max}	2.047(2)	2.043(2)
g_{int}	2.036(2)	2.027(2)
g_{min}	1.994(1)	1.989(1)

Our (somewhat less accurate) measurements of the g tensors of the other members of the series show that there is some variation between compounds in the values of the components.

E. Temperature dependence of g

It is clear from the data of Fig. 8 that the g values for $(TMTSF)_2NO_3$ are, within experimental accuracy, not dependent on temperature. The PF_6^- material, shown in Fig. 9, has all components of g decreasing with increasing temperature. Such behavior, in addition to the variation from material to material, is clearly in contradiction with the idea of a g tensor which is uniquely defined by the molecular species.

The temperature variation of the g values is more pronounced in the transition region of each material (see Figs. 8 and 9 and especially, Fig. 10). Some components turn up and some down on cooling through T_{MI}; as far as we can tell at the moment, there is no systematic trend in this variation. It does, however, reveal the development of sizable local magnetic fields at the transitions, especially those of the hexafluorides.

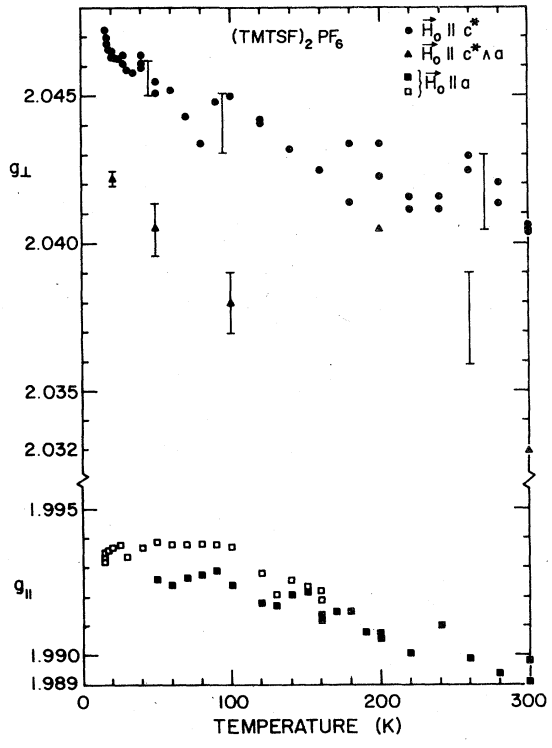

FIG. 9. Temperature dependence of the g factors of $(TMTSF)_2PF_6$ in three mutually perpendicular directions. The principal directions in the plane transverse to a are 40° away from the directions shown (see Ref. 6).

IV. DISCUSSION

A. General features

The phenomenon of conduction-electron-spin resonance in organic metals has, in the past, provided some useful insight to the electron dynamics in this class of materials. At the same time, many unsolved problems of interpretation still remain because there is, as yet, no complete theory for the g-value and relaxation rate. The pioneering work of Overhauser,[28] Elliott,[29] and Yafet,[30] who gave theories for isotropic conductors, has been frequently used as a starting point in the discussion of one-dimensional (1D) metals. Several important points have emerged from the consideration of their theories: the matrix element for one-dimensional backward scattering (k_F to $-k_F$)

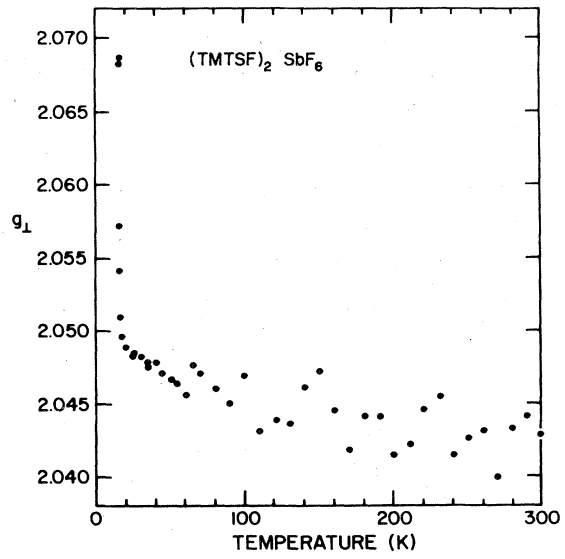

FIG. 10. Temperature dependence of a transverse g value for $(TMTSF)_2SbF_6$ showing particularly clearly the variation near T_{MI}.

accompanied by a spin-flip vanishes because of time-reversal invariance[31]; the relaxation process is therefore dominated by interchain motion which is relatively slow and hence leads to narrow lines in 1D metals relative to 3D systems with comparable spin-orbit interaction; this interchain motion is, however, fast enough to average the different g factors in two-chain organics,[16] and, therefore, to allow the decomposition of the susceptibilities on each chain.[32–35]

In this section we shall address ourselves particularly to the following features of the data: the susceptibility; the linewidth in the metallic phase of each compound, its magnitude, temperature dependence and anisotropy; and the metal-insulator transition as it is revealed in the behavior of the linewidths, g shifts, and susceptibilities. A subsection is devoted to each of these topics.

B. Spin susceptibilities

The room-temperature spin susceptibilities of all five compounds lie in the range of $2-6\times10^{-4}$ cm^3/mole.

In a simple one-electron picture the spin susceptibility is inversely proportional to the bandwidth. Assuming (as in the PF_6^- structure) two organic molecules per unit cell, but with a uniform transfer integral, $t_{\parallel}$, and one electron the molar spin susceptibility is

$$\chi_s = 2^{1/2} N_A \mu_B^2 / \pi t_{\parallel} , \tag{5}$$

where μ_B is the Bohr magneton and N_A is Avogadro's number. The susceptibilities may thus be used to compute the bandwidths as given in Table I. Clearly, the values obtained are much less than those given by thermopower[1] and plasma frequency[36] data ($4t_{\parallel} \sim 1$ eV for all compounds) implying that some magnetic enhancement mechanism is operative.

The weak metallic-phase temperature dependence of the spin susceptibility, common to all five materials, is a phenomenon which has been observed in many of the "best" organic metals,[8,13,15,16,23–26,37] especially those with symmetric organic donors and conductivity on both cation and anion chains. The origin of this temperature dependence has been a subject of considerable controversy in the past,[13] having been attributed to one-dimensional antiferromagnetic correlations,[38] the appearance of a Peierls-Fröhlich pseudogap,[15] the consequence of interchain transfer[39] or Coulomb[40] interactions, and a type of motional narrowing in the density of states.[41] Since it is apparent that the metal-insulator transition, in at least the PF_6^- and AsF_6^- (Ref. 9) derivatives, is not the simple Peierls type, it would seem that the pseudogap explanation[15] is inapplicable in this case, especially since $2k_F$ diffuse x-ray scattering is absent.[9] In these one-chain materials, interchain transfer cannot lead to a hybridization gap as it does in two-chain conductors. Hence this mechanism[39] may be immediately ruled out.

The motional narrowing argument is harder to deal with. In the analysis given by Marianer *et al.*[41] the bandwidth is reduced by a factor which depends on the mean free path, l, namely, $t_{\rm eff} = t_{\parallel} \exp(-a/l)$ where a is the lattice spacing along the chain. Since the magnitude and temperature dependence of the conductivities of all five compounds are similar we would expect similar behavior for the susceptibilities. Examination of Figs. 6 and 7 and Table I shows that although the qualitative behavior is indeed rather similar, there are significant quantitative differences. In particular, the compounds with the largest room-temperature susceptibilities (AsF_6^- and SbF_6^-) show the smallest relative changes (15 and 35%, respectively) on cooling. This is the opposite behavior to that expected from dynamic band narrowing where the room-temperature enhancement arises from a very short mean free path.

Although it is tempting to attribute the susceptibility enhancement and temperature dependence to the same mechanism in all materials, we are not able to rule out the possibility that different effects are seen in different materials. It has been shown[6,7,8,10] that the metal insulator in one or more of the TMTSF compounds is magnetic in origin. Therefore, it is natural to assume that magnetic correlations in the metallic phase are at least partly responsible for the susceptibility behavior.

C. Spin relaxation in anisotropic conductors: Linewidth

The problem of ESR linewidths and relaxation rates in organic conductors has been one of the most unyielding. Some of the difficulty may be attributed to the variation in behavior among the various materials studied: in TTF-TCNQ and most of its derivatives[15,34,42] the linewidth above the metal-insulator transition is a decreasing function of temperature; the TTF halides[43] and pseudohalides,[44] the $(TMTTF)_2X$ family[37] and the $(TMTSF)_2X$ family discussed in the present paper all have linewidths which increase with temperature; NMP-TCNQ (Ref. 45), TMTTF-TCNQ (Ref. 42), and TMTSF-DMTCNQ (Ref. 42) (NMP is N-methylphenazinium, TMTTF is tetramethyltetrathiafulvalene, DMTCNQ is dimethyl TCNQ) exhibit behavior which is a nonmonotonic function of temperature throughout the conducting temperature range. Clearly, there must be a variety of relaxation mechanisms to consider, and different materials fall into different regimes. Tomkiewicz has discussed the roles of Peierls fluctuations,[42] changing density of states[42] and dipolar interactions.[43] In the $(TMTSF)_2X$ family the data of Figs. 2 and 6 show that the

linewidth variation is much more dramatic than the density of states. Moreover, in such a highly conducting material dipole broadening will be completely narrowed out by the rapid electronic motion. Therefore, one must look for another mechanism to explain the linewidth behavior.

In the following paragraphs we shall examine the roles of the spin-orbit interaction and interchain hopping[46] from a somewhat unconventional but, we hope, useful point of view. Our model is entirely phenomenological and appeals more to physical intuition than to mathematical rigor. Nevertheless, it provides suggestive results and we hope that it might serve to stimulate a more detailed discussion of relaxation in anisotropic metals.

Consider first, the high-temperature regime: $kT > \hbar\omega_D, t_\perp$, where ω_D is the Debye frequency and $t_\perp$ is the transverse hopping integral. (For simplicity we shall assume isotropy in the plane perpendicular to the chain direction.) Motion along the chain is bandlike, whereas transverse motion is diffusive. The electrons are therefore best described by quantum numbers (k_a,i,j) where k_a is the momentum along the chain (a) direction and i and j label the chains. Scattering events for electrons with $k_a \simeq \pm k_F$ are therefore of four types: forward and backward scattering with and without an interchain hop. If the electron stays on the same chain, the initial and final momenta are precisely (anti)parallel. Since the relevant matrix elements will involve $|\vec{k}_i \wedge \vec{k}_f|$ [see, for example, Eqs. (19.4) and (19.5) of Ref. 30], forward and backward scattering on the same chain do not contribute to spin relaxation.

For interchain scattering we take a phenomenological point of view. During the scattering event the electron wave packet has orbital angular momentum about some scattering center, and the resulting orbital moment interacts with the spin via the spin-orbit interaction. One may think of the orbital motion creating an effective magnetic field, $H_{\rm eff}$, which acts on the spin.[47] Since the same interaction gives rise to the g shift, δg, of the electron from the free-spin value, one obtains

$$H_{\rm eff} \sim (\delta g/g)(\Delta/\mu_B) \ , \tag{6}$$

where Δ is a typical molecular-orbital energy difference and μ_B is the Bohr magneton. Note that the magnitude of $H_{\rm eff}$ is of order megagauss, and, since initial and final momenta are parallel to the chains, $H_{\rm eff}$ is always in the transverse plane. Moreover, $H_{\rm eff}$ will depend on the component of the g shift in the same direction in which it acts.

This enormous field only acts for a short time, namely, the "transit time" of the electron through the scattering region: $a/v_F \sim \hbar/t_\parallel$ where v_F is the Fermi velocity and $t_\parallel$ is the overlap integral along the chain. Call the mean interval between scattering events $\tau_\perp$, then the mean-square amplitude of the field is

$$\langle h^2 \rangle = H_{\rm eff}^2(\hbar/\tau_\perp t_\parallel) \ . \tag{7}$$

This is the quantity which enters the Redfield[48] theory of relaxation:

$$T_1^{-1} = \gamma_e^2 \langle h_x^2 + h_y^2 \rangle f(\omega_L) \ , \tag{8a}$$

$$T_2^{-1} = \gamma_e^2 \langle h_z^2 \rangle f(0) + \gamma_e^2 \langle h_x^2 + h_y^2 \rangle f(\omega_L) \ , \tag{8b}$$

where $f(\omega)$ is the spectral density of the fluctuating field, $\vec{h}$, and γ_e is the electron gyromagnetic ratio. Since the Larmor frequency $\omega_L \ll \hbar/t_\parallel$, $f(\omega_L) = f(0) \simeq \hbar/t_\parallel$, i.e., we are in the motionally narrowed regime.

Since the axes x,y,z are tied to the external field $\vec{H}_0$, there are two distinctly different cases: (i) $\vec{H}_0 \parallel \hat{a}$: then $\hat{z} = \hat{b}'$, $\hat{y} = \hat{c}^*$ and

$$T_1^{-1}(\parallel) = 2\gamma_e^2 \langle h^2 \rangle \hbar/t_\parallel = 2T_0^{-1} \ , \tag{9a}$$

$$T_2^{-1}(\parallel) = T_0^{-1} \ , \tag{9b}$$

where $T_0^{-1} = \gamma_e^2 H_{\rm eff}^2 (\hbar/t_\parallel)^2 (1/\tau_\perp)$ and we still ignore any anisotropy in the (b',c^*) plane. (ii) $\vec{H}_0 \perp \hat{a}$ then, e.g., $\hat{x} = \hat{a}$, $\hat{z} = \hat{c}^*$, $\hat{y} = \hat{b}'$, and

$$T_1^{-1}(\perp) = T_0^{-1} \ , \tag{10a}$$

$$T_2^{-1}(\perp) = \tfrac{3}{2} T_0^{-1} \ . \tag{10b}$$

Two extremely important points immediately emerge: in neither case is T_1 equal to T_2; and T_1 and T_2 are anisotropic, independent of the g tensor.[49]

In order to compare these results with experiment, it is necessary to estimate the scattering time $\tau_\perp$. This may be done from the transverse conductivity,[20] which in the diffusive regime is given by

$$\sigma_i = ne^2 r_i^2 / kT\tau_\perp \ , \tag{11}$$

with r_i the lattice constant in the i direction. For $(TMTSF)_2PF_6$ $\sigma_{b'} \sim 10^{-1}\ \Omega^{-1}\,\mathrm{cm}^{-1}$ and $\sigma_{c^*} \sim 10^{-1}\ \Omega^{-1}\,\mathrm{cm}^{-1}$ at room temperature, giving $\tau_\perp \sim 10^{-12}$–10^{-10} sec. From the linewidth

$$\Gamma_\perp = (\tfrac{2}{3}\gamma_e T_0)^{-1} \sim \gamma_e H_{\rm eff}^2 (\hbar/t_\parallel)^2 (1/\tau_\perp) \sim 200\ \mathrm{G} \tag{12}$$

and using $\Delta \sim 4t_\parallel \sim 1$ eV, one obtains $\tau_\perp \sim 10^{-12}$ sec in reasonable agreement with the above independent estimate. Further, the observed anisotropy in the linewidths $\Gamma(\perp)/\Gamma(\parallel) \sim 1.3$–$1.5$ are in good agreement with the model prediction of $\frac{3}{2}$. The discrepancies can easily be explained on the basis of the observed anisotropic g shift in the transverse direction and with anisotropic scattering rates. In particular note that the first term of Eq. (8b) implies a contribution to the linewidth which is proportional to square of the g shift for the same orientation of ap-

plied field. This is qualitatively what is observed: compare, for example, Figs. 5 and 8 . However, since the scattering rate $\tau_\perp$ will also be anisotropic, we feel it is unreasonable to try to extract more detailed information on the basis of such a simplistic and phenomenological model.

Insofar as the transverse conductivity[20] is temperature independent between 300 and 100 K ($\sigma_{b'}$ increases by a factor of 3, σ_{c^*} decreases by $\frac{1}{2}$) Eqs. (9)–(11) predict that the linewidths vary linearly with temperature, as observed. This is the temperature dependence which is expected for phonon-induced interchain hopping, since for $kT > \hbar\omega_D$ the phonon density is linear in temperature.

At a lower temperature the transverse motion is believed to become more bandlike and so a different behavior can be expected. The electron wave packet now propagates freely with momentum $(k_a, k_{b'}, k_{c^*})$. Further, in the absence of Kohn-anomalous $2k_F$ phonons, the density of phonons with momentum sufficient to give backward scattering will be greatly reduced below the Debye temperature. The low-temperature limiting behavior will then be proportional to T^{2n+1} where n is the power of the momentum dependence of the scattering matrix element[30]; i.e., $M_{k,k+q} \sim q^n$. The data do display a stronger temperature dependence below 100 K with T^2 to T^3 behavior depending on the range over which the power law is fit. Since there is no unique description of the data and since there is no fully quantitative theory for scattering in an anisotropic band structure, it is not fruitful to press further on this point.

D. Metal-insulator transitions

The behavior of the ESR properties in the neighborhood of the metal-insulator transition temperature, T_{MI}, may be summarized as follows: the spin susceptibilities drop very sharply, the g tensors change, the linewidth variation is different for different materials increasing for PF_6^-, AsF_6^-, SbF_6^-, remaining constant for NO_3^- and decreasing for BF_4^- as the temperature is lowered. These phenomena are in marked constrast to the behavior which is observed in the two-chain compounds TTF-TCNQ, TSeF-TCNQ (TSeF is tetraselenafulvalene), etc.,[13] which are known to undergo Peierls transitions. For them the linewidth decreases below T_{MI} (Refs. 16, 31, and 42) the susceptibility rolls off smoothly with a temperature dependence characteristically activated[15,23,24] ($E_{act} \sim 3kT_{MI}$) and any g shift is attributed[16,31–35,37–42] to changing relative susceptibilities on the two chains.

The assumption that T_{MI} represents a Peierls transition in each of these materials must, therefore, be examined more critically. Germane to this discussion are two additional measurements which have been made on $(TMTSF)_2PF_6$: there is no evidence of diffuse x-ray scattering at $2k_F$ at any temperature down to 12 K in spite of the large form factor of the Se atoms[50]; static susceptibility data[8,10,51] show that the low-temperature phase is magnetic, i.e., that the spin susceptibility does not vanish at zero temperature as it does for a Peierls semiconductor. These facts have led to the suggestion[7,8] that T_{MI} is a spin-density-wave (SDW) transition rather than a Peierls or charge-density-wave (CDW) transition.

The ESR data in the PF_6^-, AsF_6^-, and SbF_6^- compounds tend to support this hypothesis. The large g shift and abrupt linewidth increase at T_{MI} indicate the development of local internal magnetic fields as expected when a magnetic moment localizes in each unit cell. The disappearance of the ESR signal can then be explained in terms of either a very broad line characteristic of a one-dimensional antiferromagnet well below its mean-field temperature or a shifted oscillator strength to an antiferromagnetic resonance (AFMR) as in a three-dimensional ordered antiferromagnet. It is difficult to make quantitative any part of this description, since there are no available ESR (or AFMR) data in the low-temperature phase. However, using typical values for the relevant exchange $J \sim t^2/U \sim 1000$ K, and dipole anisotropy $D \sim \mu_B^2/a^3 \sim 10^{-3}$ K which enter the AFMR frequency, ω_{AFMR} and spin-flop fields, H_{sf}

$$\hbar\omega_{AFMR} \sim \mu_B H_{sf} \sim \sqrt{JD} \tag{13}$$

yields $H_{sf} \sim 10^4$ G. This is the same order of magnitude as the onset of nonlinearity which is seen in the static susceptibility[8,10] (6 kG) and implies that one branch of the field-dependent AFMR ought to be accessible. Whether it is visible in a standard cavity absorption experiment depends on its width.

A possible hypothesis for the appearance of the two distinct transitions seen in our samples at 17 ± 2 K in transport measurements[1,20] and ESR and at 11.5 K in the static susceptibility[8] is then as follows. The higher temperature represents the onset of a one-dimensional spin-density wave due to the localization of some fraction of a magnetic moment at each site. There is no long-range magnetic order, but there is still a true phase transition because of the $4k_F$ CDW which accompanies the $2k_F$ SDW. Since $4k_F = a^*$ the structural transition is not visible in x-ray scattering as a superlattice, but corresponds rather to the redistribution of charge within the original unit cell. The exchange potential, with periodicity $2k_F$, opens a single-particle gap at the Fermi surface for both up and down spins and causes the semiconducting transport behavior.[52] The ESR line broadens beyond observability but the change in the static susceptibility is small, proportional to the amplitude of the SDW.

Within this hypothetical picture the 11.5 K transi-

tion would be identified as the 3D ordering temperature of the magnetism: T_N. Below T_N the magnetic response is nonlinear due to spin-flop behavior.

A problem arises because of the different behavior observed in other laboratories. Chaikin *et al.*[53] observe a resistive anomaly at 13 K, compared to the 15–19 K range seen by Bechgaard *et al.*[1,20] Walsh *et al.* initially reported the disappearance of the ESR line below 15 K,[7] but, in more recent work[51] with presumably purer samples now quote 11 K. Tomkiewicz and co-workers[54] find the metal-insulator transition to be at 12 K and to rise rapidly on alloying with TMTTF. Clearly then the properties of $(TMTSF)_2PF_6$ are extremely dependent on the presence of defects, impurities and/or slight nonstoichiometry. The question of whether the existence of an intermediate phase, as we have observed, is stabilized or suppressed by such imperfections must remain open until more systematic study has been performed.

V. SUMMARY

The family of organic conductors $(TMTSF)_2X$ has been found to possess generally similar ESR properties: a g tensor typical of the TMTSF cation, a linewidth which increases monotonically with temperature in the metallic phase, an intensity which is weakly temperature dependent above T_{MI} and vanishes below it. There are, however, several very distinct differences in detail among the various members of the family. The hexafluorides have a temperature-dependent g tensor, even in the metallic state; their linewidths increase sharply on cooling through T_{MI} whereas no rapid changes are seen in the nitrate linewidth and that of the perfluoroborate decreases. These differences lead us to believe that while the materials are generally similar there are subtle differences in bandwidth, electron-electron interactions, electron-phonon interactions, and interchain coupling. Hence the family provides a series of crystalline materials which may be used to examine the predictions of the various theories of the 1D Fermi gas.[55]

The anisotropy in the linewidth $\Gamma_\perp/\Gamma_\parallel \sim 1.3-1.5$ can be understood semiquantitatively in terms of a phenomenological model of interchain hopping and spin-orbit coupling. This model predicts a difference between T_1 and T_2 in such anisotropic metals, as well as different ratios $T_1(\parallel)/T_1(\perp)$ and $T_2(\parallel)/T_2(\perp)$. It will be amusing to explore these predictions in suitable one-dimensional materials (i.e., those with narrower ESR lines than those reported here).

The metal-insulator transition [especially in $(TMTSF)_2PF_6$] has been discussed in terms of a spin-density-wave instability. Many features of the data are at least quantitatively explained by such a description, whereas a Peierls (or CDW) transition is almost certainly ruled out. Recent theoretical work[56,57] has shown that a quasi-1D Fermi gas which has moderate interchain hopping is the most likely candidate for a SDW instability. The optical properties[36] of $(TMTSF)_2PF_6$ and the modest pressures required to stabilize the metallic state[2] imply that the transverse bandwidth is indeed significant in this material. Whether these same material parameters imply that the superconducting state is triplet[55,57] in nature is an intriguing question.

Another area which requires further examination is whether the nature of the metal-insulator transitions is the same for all materials. The PF_6^-, AsF_6^-, and SbF_6^- compounds certainly appear to be similar, but the static susceptibility behavior remains to be checked. The different temperature dependence of the linewidth for NO_3^- and BF_4^- is puzzling in view of the equally rapid disappearance of ESR intensity.

ACKNOWLEDGMENTS

H. J. P. thanks the Danish Research Council for support during his visit to Cornell University. J. C. S. acknowledges partial support from the Cornell Materials Science Center under the NSF-MRL program, Grant No. DMR 76-81083. The authors are grateful for useful and stimulating discussions with Professor R. H. Silsbee and Professor J. W. Wilkins.

---

*Present address: Physics Laboratory III, Technical Univ. of Denmark, DK-2800, Lyngby, Denmark.

†Present address: IBM Research, 5600 Cottle Rd., San Jose, Calif. 95193.

[1]K. Bechgaard, C. S. Jacobsen, K. Mortensen, H. J. Pedersen, and N. Thorup, Solid State Commun. 33, 1119 (1980).

[2]D. Jerome, A. Mazaud, M. Ribault, and K. Bechgaard, J. Phys. (Paris) Lett. 41, L95 (1980).

[3]M. Ribault, G. Benedek, D. Jerome, and K. Bechgaard, J. Phys. (Paris) Lett. 41, L397 (1980).

[4]R. L. Greene and E. M. Engler, Phys. Rev. Lett. 45, 1587 (1980).

[5]K. Andres, F. Wudl, D. B. McWhan, G. A. Thomas, D. Nalewajek, and A. L. Stevens, Phys. Rev. Lett. 45, 1449 (1980).

[6]H. J. Pedersen, J. C. Scott, and K. Bechgaard, Solid State Commun. 35, 207 (1980).

[7]W. M. Walsh, F. Wudl, G. A. Thomas, D. Nalewajek, J. J. Hauser, P. A. Lee, and T. Poehler, Phys. Rev. Lett. 45, 829 (1980).

[8]J. C. Scott, H. J. Pedersen, and K. Bechgaard, Phys. Rev.

Lett. 45, 2125 (1980).
[9]M. Ribault, J.-P. Pouget, D. Jerome, and K. Bechgaard, J. Phys. (Paris) Lett. 41, L607 (1980).
[10]K. Mortensen, Y. Tomkiewicz, T. D. Schultz, and E. M. Engler (unpublished).
[11]N. Thorup, G. Rindorf, H. Soling, and K. Bechgaard, Acta Crystallogr. B (in press).
[12]N. Thorup, G. Rindorf, and H. Soling (private communication).
[13]For recent reviews see *Highly Conducting One-Dimensional Solids,* edited by J. T. Devreese, R. P. Evrard, and V. E. van Doren (Plenum, New York, 1979); or *The Physics and Chemistry of Low Dimensional Solids,* edited by L. Alcacer (Reidel, Dordrecht, Holland, 1980).
[14]K. Bechgaard, D. O Cowan and A. N. Bloch, J. Chem. Soc. Chem. Commun. 937 (1974).
[15]J. C. Scott, A. F. Garito, and A. J. Heeger, Phys. Rev. B 10, 3131 (1974).
[16]Y. Tomkiewicz, B. A. Scott, L. J. Tao, and R. S. Title, Phys. Rev. Lett. 32, 1363 (1974).
[17]W. M. Walsh, L. W. Rupp, D. E. Schafer, and G. A. Thomas, Bull. Am. Phys. Soc. 19, 296 (1974).
[18]F. J. Dyson, Phys. Rev. 98, 349 (1955).
[19]The general case is discussed in detail by A. H. Kahn, J. Appl. Phys. 46, 4965 (1975).
[20]C. S. Jacobsen, K. Mortensen, M. Weger, and K. Bechgaard, Solid State Commun. (in press).
[21]N. Bloembergen, J. Appl. Phys. 23, 1383 (1952).
[22]L. I. Buravov, O. N. Eremenko, R. B. Lyobovskii, L. P. Rozenberg, M. L. Khidekel, R. P. Shibaeva, I. F. Shchegolev, and E. B. Yagubskii, Zh. Eksp. Teor. Fiz. Pis'ma Red. 20, 457 (1974) [Sov. Phys. JETP Lett. 20, 208 (1974)].
[23]J. Gulley and J. F. Weiher, Phys. Rev. Lett. 34, 1061 (1975).
[24]J. C. Scott, S. Etemad, and E. M. Engler, Phys. Rev. B 17, 2269 (1978).
[25]P. Delhaes, S. Flandrois, J. Amiell, G. Keryer, E. Toreilles, J. M. Fabre, L. Giral, C. S. Jacobsen, and K. Bechgaard, Ann. N. Y. Acad. Sci. 313, 467 (1978).
[26]G. Soda, D. Jerome, M. Weger, J. M. Fabre, L. Giral, and K. Bechgaard, in *Proceedings of the Conference on Organic Conductors and Semiconductors, Siofok, Hungary, 1976,* edited by L. Pal, G. Gruner, A. Janossy, and J. Solyom (Springer-Verlag, Berlin, 1977), p. 371.
[27]W. M. Walsh, L. W. Rupp, F. Wudl, M. L. Kaplan, D. E. Schafer, G. A. Thomas, and R. Gemmer, Solid State Commun. 33, 413 (1980).
[28]A. W. Overhauser, Phys. Rev. 89, 689 (1953).
[29]R. J. Elliott, Phys. Rev. 96, 266 (1954).
[30]Y. Yafet, in *Solid State Physics,* edited by F. Seitz and D. R. Turnbull (Academic, New York, 1963), Vol. 14, p. 1.
[31]Y. Tomkiewicz, E. M. Engler, and T. D. Schultz, Phys. Rev. Lett. 35, 456 (1975).
[32]Y. Tomkiewicz, A. R. Taranko, and J. B. Torrance, Phys. Rev. Lett. 36, 751 (1976); Phys. Rev. B 15, 1017 (1977).
[33]Y. Tomkiewicz, B. Welber, P. E. Seiden, and R. Schumaker, Solid State Commun. 23, 471 (1977).
[34]Y. Tomkiewicz, A. R. Taranko, and R. Schumaker, Phys. Rev. B 16, 1380 (1977).
[35]A criticism of the decomposition method is given by E. Conwell, Phys. Rev. B 22, 3107 (1980). A rebuttal is presented by Y. Tomkiewicz, A. R. Taranko, and J. B. Torrance, *ibid.* 22, 3113 (1980).
[36]C. S. Jacobsen, D. B. Tanner, and K. Bechgaard (unpublished).
[37]P. Delhaes, C. Copulon, J. Amiell, S. Flandrois, E. Toreilles, J. M. Fabre, and L. Giral, Mol. Cryst. Liq. Cryst. 50, 43 (1979).
[38]J. B. Torrance, Y. Tomkiewicz, and B. D. Silverman, Phys. Rev. 15, 4738 (1977).
[39]U. Bernstein, P. M. Chaikin, and P. Pincus, Phys. Rev. Lett. 34, 271 (1975).
[40]P. A. Lee, T. M. Rice, and R. A. Klemm, Phys. Rev. B 15, 2984 (1977).
[41]S. Marianer, M. Weger, and H. Gutfreund (unpublished).
[42]Y. Tomkiewicz, Phys. Rev. B 19, 4038 (1979).
[43]Y. Tomkiewicz and A. R. Taranko, Phys. Rev. B 18, 733 (1978).
[44]R. B. Somoano, A. Gupta, V. Hadek, M. Novotny, M. Jones, T. Datta, R. Deck, and A. M. Hermann, Phys. Rev. B 15, 595 (1977).
[45]A. J. Epstein, S. Etemad, A. F. Garito, and A. J. Heeger, Phys. Rev. B 5, 952 (1972).
[46]This is the same mechanism discussed for example in Refs. 16 and 31.
[47]In quantum-mechanical language the scattering process involves admixture into the electron wave packet excited molecular states. These are the same states which the spin-orbit interaction mixes into the ground state.
[48]A. G. Redfield, IBM J. Res. Dev. 1, 19 (1957). See also C. P. Slichter, *Principles of Magnetic Resonance,* 2nd ed. (Springer-Verlag, Berlin, 1978), p. 179. [Note that Eq. (5.210) contains a misprint.]
[49]In the isotropic case, where $\langle h_x^2 \rangle = \langle h_y^2 \rangle = \langle h_z^2 \rangle$ and the scattering is from one part of the Fermi sphere to another, Eqs. (9) and (10) reduce to the standard results of Elliott (Ref. 29) and Yafet (Ref. 30).
[50]J.-P. Pouget, Chem. Scr. (in press).
[51]F. Wudl, F. J. diSalvo, and W. M. Walsh (private communication).
[52]A. W. Overhauser, Phys. Rev. Lett. 4, 462 (1960); Phys. Rev. 128, 1437 (1962).
[53]P. M. Chaikin, G. Gruner, E. M. Engler, and R. L. Greene, Phys. Rev. Lett. 45, 1874 (1980).
[54]Y. Tomkiewicz (private communication).
[55]J. Solyom, Adv. Phys. 28, 201 (1979).
[56]Y. Suzumara and H. Fukuyama, J. Low Temp. Phys. 31, 273 (1978).
[57]For a review see T. M. Rice, in *Proceedings of the Conference on One-Dimensional Physics, Fribourg, Switzerland, 1980,* edited by J. Bernasconi and T. Schneider (Springer-Verlag, Berlin, 1981).